Solving the heliogyro's inverse problem

Heiligers, Jeannette; Guerrant, D.; Lawrence, D

DOI
10.2514/6.2016-5334

Publication date
2016

Document Version
Accepted author manuscript

Published in
AIAA/AAS Astrodynamics Specialist Conference

Solving the Heliogyro's Inverse Problem

Jeannette Heiligers*
Delft University of Technology, Kluyverweg 1, 2629 HS Delft, the Netherlands
University of Colorado, Boulder, CO 80309, USA

Daniel Guerrant†
Deep Space Systems Inc, Littleton, CO 80127, USA

Dale Lawrence‡
University of Colorado, Boulder, CO 80309, USA

A heliogyro is a solar sail concept that divides the solar sail membrane into a number of long, slender blades of film extended from a central hub, maintained in a flat state through spin-induced tension. The heliogyro can redirect and scale the solar radiation pressure (SRP) force and can achieve attitude control by twisting the blades, similar to a helicopter rotor. Different pitch profiles exist, including pitching the blades in a collective, cyclic or combined collective and cyclic manner. While the forward mapping, i.e., computing the SRP force and moment generated by the heliogyro for a given pitch profile, is straightforward, the inverse of the problem is much more complex. However, this inverse problem (finding the blades' pitch that results in a desired SRP force and/or moment) is crucial for heliogyro mission design and operations. This paper therefore solves the inverse problem numerically: first, only for a desired SRP force or SRP moment and subsequently for the fully coupled inverse problem. The developed methods are subsequently applied to track a reference trajectory that corrects for injection errors into a solar sail Sun-Earth sub-L_1 halo orbit.

I. Introduction

Research into solar sailing as well as previous and future solar sail initiatives (IKAROS (JAXA, 2010), NanoSail-D2 (NASA, 2010), Lightsail-1 (The Planetary Society, 2015), and NEA Scout§ (NASA)) are driven by the huge potential of solar sail missions that are not constrained by propellant mass [1, 2]: solar sailing exploits the radiation pressure generated by solar photons that reflect off a large, highly reflective membrane to produce continuous thrust.

* Marie Curie Research Fellow, Faculty of Aerospace Engineering. AIAA Member.
† Senior Engineer, Deep Space Systems Inc., 8341 Sangre De Cristo Rd Suite 205, Littleton, CO 80127.
‡ Professor, Aerospace Engineering Sciences, ECAE-197, 429 UCB. Associate Fellow AIAA.
§ Jet Propulsion Laboratory/California Institute of Technology, Near Earth Asteroid Scout (NEAScout), http://www.jpl.nasa.gov/cubesat/missions/neascout.php, accessed February 22, 2016

With the Sun as 'propellant' source, solar sail missions have in principle infinite lifetime and can build up vast quantities of ΔV over that mission lifetime, enabling high-energy and long-duration missions [3].

While traditional solar sails adopt a flat (either square- or disc-shaped) configuration, renewed interest exists in the heliogyro concept [4, 5]. The heliogyro divides the reflective membrane into several long blades and by slowly spinning, the blades are maintained in a flat state. The spin-induced flattening removes the need for a relatively heavy mechanical deployment and stiffening structure as required for the flat sail configuration. The heliogyro concept is therefore more efficient, allowing a higher force per unit mass because of a lower sail loading (the spacecraft mass-to-sail-area ratio). In addition, while the thrust acceleration of a flat sail is fully prescribed by the sail's attitude with respect to the Sun, the heliogyro can scale down the acceleration in any direction (away from the Sun) by pitching its blades [6].

Different blade pitch profiles exist, including collective and cyclic profiles or a combination of the two [4, 7, 8]. The collective pitch profile applies a constant and equal pitch to each of the blades whereas the cyclic pitch profile sinusoidally changes the blades' pitch over one or two rotational periods of the heliogyro. The case of a sinusoidally changing pitch over two rotational periods is referred to as the half-p pitch profile. Besides the amplitudes of these three pitch profiles, the cyclic and half-p profiles also have a phase angle. Therefore, this paper uses a total of five pitch controls to determine fully the heliogyro's SRP force and moment at a specific attitude with respect to the Sun. Obtaining the SRP force and moment is straightforward as both can be explicitly written as a function of the pitch controls [7]. Except for a few very specific and simplistic cases, however, the problem cannot be analytically inverted, i.e. given a specific SRP force and/or moment, the pitch controls that enable that force and moment cannot be derived analytically and must be determined numerically.

The need for a numerical solution method is especially evident from the fact that the fully coupled problem is over-determined as it uses a maximum of five controls for a total of six degrees of freedom. Another issue with the inverse problem is the choice of the controls, i.e., which controls are selected to generate the desired moment and which ones are allocated to the generation of the required force? Furthermore, the numerical nature of the problem introduces the difficulty that a solution can only be found if a solution indeed exists. It is important to note that a heliogyro can, for example, only generate forces that are constrained to the volume of a bubble around the Sun-sail line. A related issue is the fact that the momentum transferred by the solar photons to the heliogyro needs to be divided over the force and moment generating capabilities of the sail. For example, generating the moment required to reorient the heliogyro reduces the SRP force available for orbital maneuvering. This further restricts the force and moment combinations for which a solution to the inverse problem exists.

This paper addresses all these issues and defines a numerical approach to solving the inverse problem, finding the pitch controls to enable either a desired force, a desired moment, or a fully coupled force and moment. One of the few inputs required for the numerical method is an initial guess for the pitch controls, which are all angles. The performance of the numerical method is then expressed through how good this initial guess needs to be in order for the method to converge to a solution. This paper shows that, in many cases, the initial guess can be quite poor (i.e., far from the solution), on the order of tens of degrees, providing a robust approach for solving the inverse problem. Finally, after

applying the developed method to randomly selected forces and/or moments, the approach is applied to track a reference trajectory that has previously been developed to correct for injection errors into a solar sail Sun-Earth sub-L_1 halo orbit [6, 9].

II. Heliogyro force and moment models

This paper assumes an ideal solar sail reflectance model [1, 2] that considers the heliogyro blades to be perfectly reflecting and perfectly flat, without wrinkles or optical imperfections. Under these assumptions, the incoming solar photons are specularly reflected and the solar radiation pressure force and acceleration act perpendicular to the heliogyro blade. To define the forces and moments generated by the heliogyro, a set of reference frames is involved (see Figure 1), with their transformations detailed in the Appendix of References [6, 9]. This paper expresses the SRP force produced by the heliogyro in the Sun coordinate system $S\left(\hat{\mathbf{s}},\hat{\mathbf{l}},\hat{\mathbf{p}}\right)$ and the SRP moment in the despun coordinate system $D\left(\hat{\mathbf{d}}_1,\hat{\mathbf{d}}_2,\hat{\mathbf{d}}_3\right)$. In the Sun coordinate system, $\hat{\mathbf{s}}$ is the Sun-sail unit vector, $\hat{\mathbf{l}}=\left(\hat{\mathbf{z}}\times\hat{\mathbf{s}}\right)/\left|\hat{\mathbf{z}}\times\hat{\mathbf{s}}\right|$ where $\hat{\mathbf{z}}$ is the unit vector perpendicular to the Earth's orbital plane, and $\hat{\mathbf{p}}$ completes the right-handed reference frame. In the despun coordinate system, $\hat{\mathbf{d}}_1$ is along the heliogyro spin axis, $\boldsymbol{\Omega}$, $\hat{\mathbf{d}}_3$ is along blade 1 at time $t=0$ (where the orientation of blade 1 at $t=0$ is defined by the heliogyro's clock angle, γ, with respect to $\hat{\mathbf{p}}$), and $\hat{\mathbf{d}}_2$ completes the right handed reference frame. The despun reference frame is thus defined at time $t=0$ and remains fixed relative to the Sun coordinate system, $S\left(\hat{\mathbf{s}},\hat{\mathbf{l}},\hat{\mathbf{p}}\right)$, for given heliogyro attitude angles η (cone angle) and γ (clock angle), while the heliogyro rotates around the heliogyro spin-axis. Reference [7] expresses the averaged SRP force and moments in these reference frames as:

$$\mathbf{F}_S=\frac{2AP}{4\pi}\left[SD\right]\int_0^{4\pi}\operatorname{sign}\left(s_{L_i,3}\right)\left(s_{L_i,3}\right)^2\begin{bmatrix}\cos\theta_i\\ \sin\theta_i\sin\psi_i\\ -\sin\theta_i\cos\psi_i\end{bmatrix}d\psi_i \tag{1}$$

$$\mathbf{M}_D=\frac{APR}{4\pi}\int_0^{4\pi}\operatorname{sign}\left(s_{L_i,3}\right)\left(s_{L_i,3}\right)^2\begin{bmatrix}-\sin\theta_i\\ \cos\theta_i\sin\psi_i\\ -\cos_i\cos\psi_i\end{bmatrix}d\psi_i\,. \tag{2}$$

In Eqs. (1) and (2), P is the solar radiation pressure (4.563×10^{-6} N/m^2 at 1 Astronomical Unit (AU) [1]), A is the total heliogyro blade area, R is the heliogyro blade radius, $s_{L_i,3}$ is the component of the Sun vector, $\hat{\mathbf{s}}$, normal to the i^{th} blade and expressed in the i^{th} blade coordinate system ($L_i\left(\hat{\mathbf{l}}_1,\hat{\mathbf{l}}_2,\hat{\mathbf{l}}_3\right)$, see Figure 1c), and ψ_i is the i^{th} blade azimuth angle in the spin plane (see Figure 1b for the first blade). Furthermore, $\left[SD\right]=R_1\left(\gamma\right)R_3\left(\eta\right)$ is the rotation matrix that translates a vector in the $D\left(\hat{\mathbf{d}}_1,\hat{\mathbf{d}}_2,\hat{\mathbf{d}}_3\right)$-frame to the $S\left(\hat{\mathbf{s}},\hat{\mathbf{l}},\hat{\mathbf{p}}\right)$-frame. Finally, θ_i is the individual blade's pitch angle, which is elaborated upon below. First note that, because the heliogyro rotates, the SRP force and moment vectors change as the heliogyro spins. They are therefore averaged over two revolutions (in case the selected blade

pitch profile includes half-p) through the integrals in Eqs. (1) and (2) and the subsequent division by 4π. Because the integral is the same for each blade, the average acceleration for all blades can be obtained by evaluating the integral for one blade only (i.e., i in Eqs. (1) and (2) can be set to $i=1$) and multiplying by the total blade area, A. Note that only very specific cases allow for the integrals in Eqs. (1) and (2) to be evaluated analytically (see Section III) and are therefore evaluated numerically in most cases.

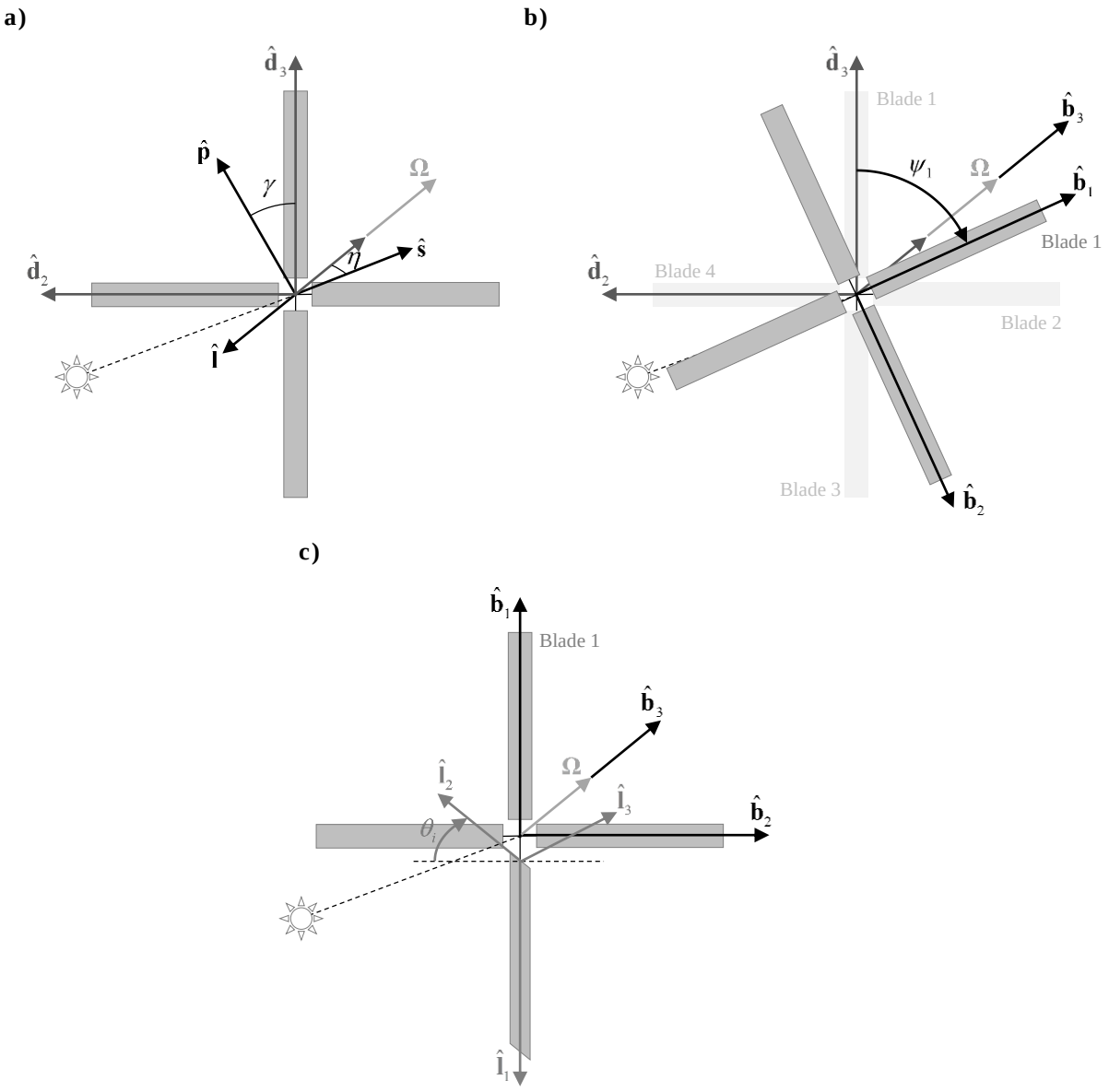

Figure 1 Definition of reference frames [9]. a) S **- and** D **-frames. b)** D **- and** B **-frames. c)** B **- and** L_i **- frames.**

As mentioned below Eq. (2), θ_i is the blade's pitch angle, and its value depends on the pitch profile selected. Reference [4] and many following works (e.g. References [5, 7-9]) define three different pitch profiles, which can be used independently or in combination: the collective profile ('Co'), ½-period cyclic profile (half-p, 'HP'), and the 1-period cyclic profile (cyclic, 'Cy'). The collective profile pitches the blades at a constant value, equal for all blades, while the heliogyro rotates, whereas the half-p and cyclic profiles pitch the blades sinusoidally with revolution. While the half-p profile repeats after two revolutions (requiring the force and moment vectors in Eqs. (1) and (2) to be averaged over two revolutions), the cyclic profile repeats after one revolution. Each of the pitch profiles and its effect on the solar radiation pressure force and moment is illustrated in Figure 2, which is taken from Reference [7]. In the example of a Sun-facing heliogyro (with $\eta = 0$), the collective and half-p profiles only generate a force along the Sun direction (or equivalently, along the spin axis), while the cyclic profile can also generate a force component in the plane perpendicular to the Sun-sail line. Note that the latter is a unique capability of the heliogyro compared with traditional, flat solar sails. In the Sun-facing case, the collective profile allows a spin-up or spin-down of the heliogyro, the half-p profile allows attitude changes, and the cyclic profile generates no moment. Note that, while these force and moment generating capabilities change when considering different attitudes of the sail (i.e., $\eta \neq 0$), a purely cyclic profile never generates a net moment. This capability is exploited in Section VIII.

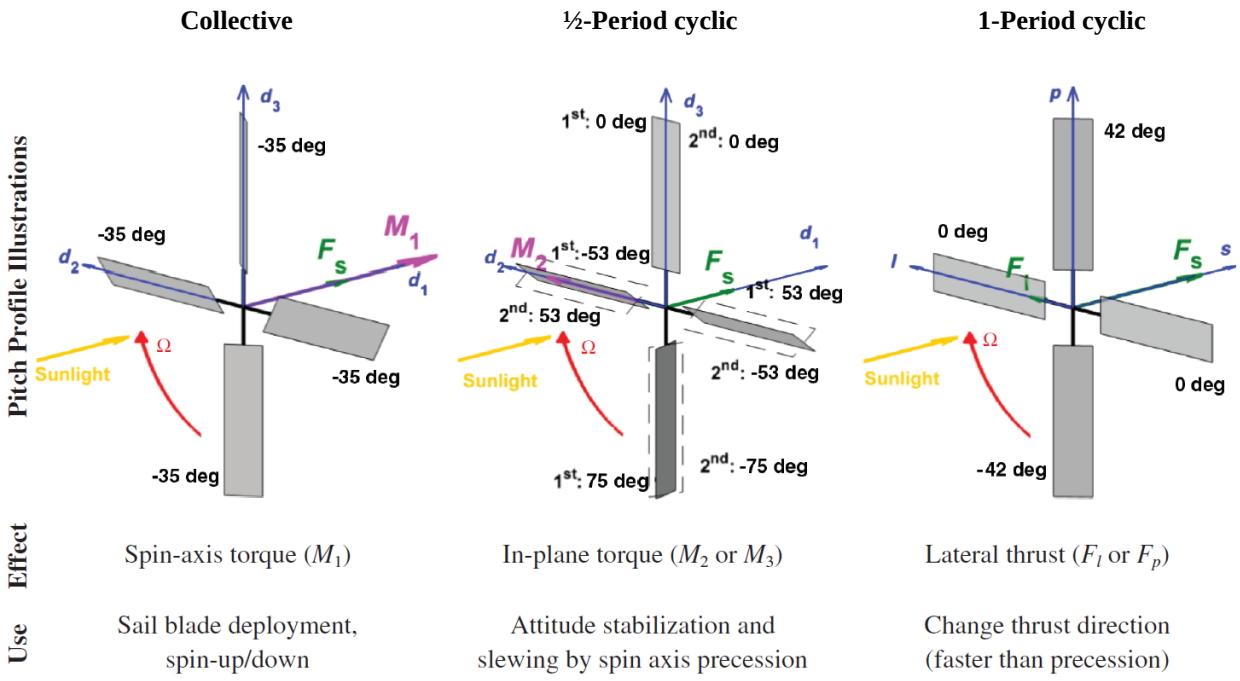

Figure 2 Illustration of pitch profiles for Sun-facing heliogyro ($\eta = 0$) (source: [7]).

For use in Eqs. (1) and (2) the actual pitch angle of each blade needs to be known and is given by Reference [7] for any combination of the three pitch profiles described above:

$$\theta_i = -a_{co} + a_{hp} \sin\left[\frac{1}{2}\left(\psi_i - \phi_{hp} - \text{sign}\left(a_{hp}\right)\frac{\pi}{2}\right)\right] + a_{cy} \sin\left(\psi_i - \phi_{cy}\right) \tag{3}$$

where a_{co}, a_{hp}, and a_{cy} are the amplitudes of the collective, half-p and cyclic profiles, respectively, and ϕ_{hp} and ϕ_{cy} are the phase angles of the half-p and cyclic profiles, respectively. Equations (1)-(3) combined provide the forward mapping from blade pitch controls to the resultant SRP force and moment.

To demonstrate the force and moment generating capabilities of the heliogyro, Figure 3a and Figure 4a show the *spin-averaged* force contours (and Figure 3b the moment contours around the $\left(\hat{\mathbf{d}}_1, \hat{\mathbf{d}}_2\right)$-axes for the collective profile) of equal pitch amplitudes for a collective and cyclic profile, respectively. Each curve represents one specific amplitude of either the collective or cyclic profiles and is constructed by considering heliogyro attitudes of $\eta = \left[-90^o, 90^o\right]$ and assuming that the clock angle γ equals zero. Extending the results to non-zero values for γ yields the three-dimensional force curves of Figure 3c, d and Figure 4b. The figure shows that a non-zero γ angle rotates the two-dimensional "bubble-shaped" force curves around the $\hat{\mathbf{s}}$-axis (Sun-sail line). Note that the moment generated by the collective profile is not affected by a non-zero value for the angle γ and will always produce a moment along the $\hat{\mathbf{d}}_1$- and $\hat{\mathbf{d}}_2$-axes only. As concluded in previous works [6, 9], the results in Figure 3 and Figure 4 show that a heliogyro can fill up a force bubble volume around the Sun-sail line through appropriate choices for the pitch profile, while a traditional flat sail can only generate forces that are constrained to the surface of that bubble. The authors previously demonstrated this unique capability of the heliogyro to provide superior orbital control capabilities compared to a flat sail configuration when correcting for injection errors or solar sail deployment delays upon injection into solar sail Sun-Earth sub-L_1 halo orbits [6, 9].

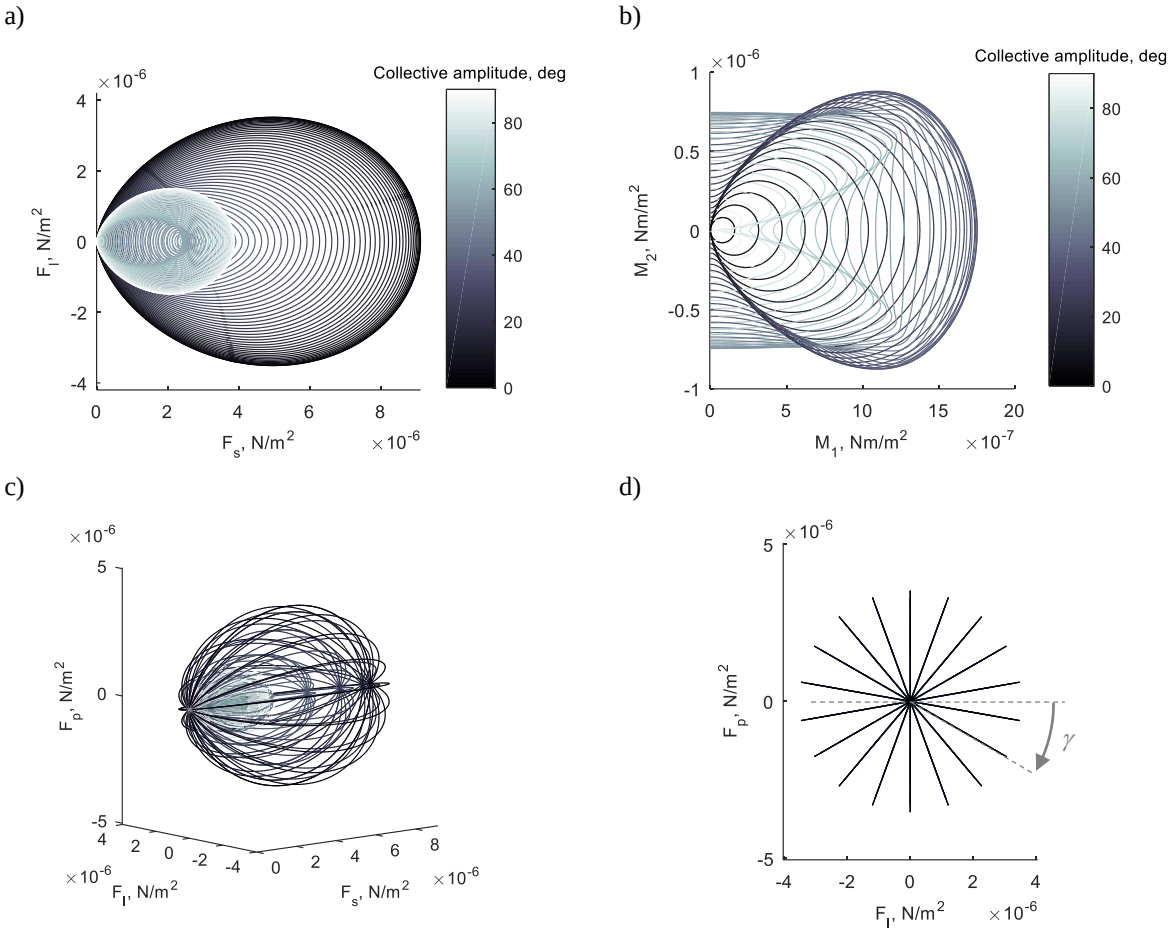

Figure 3 Spin-averaged SRP force and moment per square meter sail area and meter blade radius for a collective pitch profile at 1 AU. a-b) For η = [-90°, 90°] and γ = 0°. c-d) For η = [-90°, 90°] and γ = [-90°,90°].

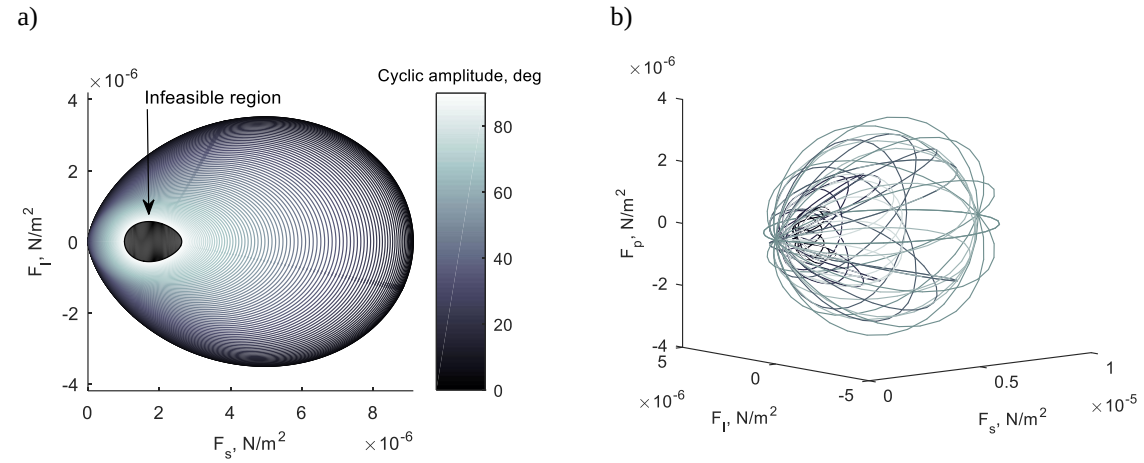

Figure 4 Spin-averaged SRP force per square meter sail area and meter blade radius for a cyclic pitch profile (ϕ_{Cy} = 0°) at 1 AU. a) For η = [-90°, 90°] and γ = 0°. b) For η = [-90°, 90°] and γ = [-90°, 90°].

III. Analytical solution to inverse problem

Section II and particularly Eqs. (1) and (2) show that the forward mapping from blade pitch controls to the resulting SRP force and moment is straightforward. The inverse of the problem, finding the blade pitch controls required to produce a desired force and/or moment, is, however, far from straightforward. The main reason for this is that the integral in Eqs. (1) and (2) cannot be evaluated analytically for a generic pitch profile in Eq. (3) and even if an analytical solution to the integral would exist, the discrepancy between the number of controls (five at maximum: a_{Co}, a_{HP}, ϕ_{HP}, a_{Cy} and ϕ_{Cy}) and number of equations (between one and six) does not always allow an analytical expression of the inverse problem. Only in *very* specific cases does an analytical solution to the inverse problem exist [10]. For example, when considering a collective profile and a Sun-facing attitude of the heliogyro ($\eta = \gamma = 0^o$), the resulting force and moment can be computed analytically from Eqs. (1) and (2). The result of this forward mapping is:

$$\mathbf{F}_S = \begin{bmatrix} f_s & f_l & f_p \end{bmatrix} = \begin{bmatrix} 2AP\cos^3(a_{Co})\,\mathrm{sign}\left(\cos\left[a_{Co}\right]\right) & 0 & 0 \end{bmatrix} \tag{4}$$

$$\mathbf{M}_D = \begin{bmatrix} M_{d_1} & M_{d_2} & M_{d_3} \end{bmatrix} = \begin{bmatrix} APR\cos^2(a_{Co})\,\mathrm{sign}\left(\cos\left[a_{Co}\right]\right)\sin(a_{Co}) & 0 & 0 \end{bmatrix} \tag{5}$$

With one control, a_{Co}, and two equations, the analytical inverse mapping can only satisfy either the force or the moment. When considering only the force, the inverse mapping provides four solutions, i.e., four collective pitch amplitudes that provide the same SRP force along the Sun-sail line:

$$a_{Co} = \pm\cos^{-1}\left(\pm 2^{-\frac{1}{3}}\left[f_s/(AP)\right]^{\frac{1}{3}}\right) \tag{6}$$

When considering only the moment, the inverse mapping provides six solutions. For conciseness, only one solution is provided here:

$$a_{Co} = -\cos^{-1}\left(-\frac{1}{\sqrt{6}}\left(\sqrt{2+\frac{2^{\frac{4}{3}}\xi^4+\left(-54\xi^4M_{d_1}^2+4\xi^6+6\sqrt{-12\xi^{10}M_{d_1}^2+81\xi^8M_{d_1}^4}\right)^{\frac{2}{3}}}{\xi^2\left(-27\xi^4M_{d_1}^2+2\xi^6+3\sqrt{-12\xi^{10}M_{d_1}^2+81\xi^8M_{d_1}^4}\right)^{\frac{1}{3}}}}\right)\right) \text{ with } \xi = APR \tag{7}$$

While Eqs. (6) and (7) provide closed-form solutions for the collective, Sun-facing case, analytical solutions only exist for very few other cases when moving away from the Sun-facing condition or when considering profiles other than the collective [10].

IV. Numerical approach to inverse problem

When no analytical solution to the inverse problem exists, a numerical approach is required to find the blade pitch controls, $\hat{\mathbf{x}} \in \left[a_{Co}, a_{HP}, \phi_{HP}, a_{Cy}, \phi_{Cy}\right]$, that provide a desired force, $\mathbf{F}_0 = \begin{bmatrix} F_{0,s} & F_{0,l} & F_{0,p} \end{bmatrix}^T$, and/or moment, $\mathbf{M}_0 = \begin{bmatrix} M_{0,d_1} & M_{0,d_2} & M_{0,d_3} \end{bmatrix}^T$. The system of non-linear equations to solve is thus:

$$\begin{aligned} \mathbf{F}_S\left(\hat{\mathbf{x}}\right) &= \mathbf{F}_0 \\ \mathbf{M}_D\left(\hat{\mathbf{x}}\right) &= \mathbf{M}_0 \end{aligned}. \tag{8}$$

Here, the algorithms implemented in Matlab®'s *fsolve.m* function are used to solve the system in Eq. (8). The authors used the 'Trust region dogleg' algorithm for square systems and the 'Levenberg-Marquardt' algorithm otherwise, with their options set as *optimset('TolX',10^-10,'TolFun',10^-10,'MaxFunEval',1000,'MaxIter',1000)*. The only necessary input for these algorithms is the system of nonlinear equations in Eq. (8) and an initial guess for the blade pitch controls, $\hat{\mathbf{x}}_0$. A schematic of the core of the numerical approach is provided by the black elements in Figure 5: an initial guess, $\hat{\mathbf{x}}_0$, is provided to the solver and the force and moment corresponding to this initial guess, $\hat{\mathbf{F}}$ and $\hat{\mathbf{M}}$, are computed through a forward mapping using Eqs. (1)-(3). These resulting force and moment are compared to the desired force and moment, $\mathbf{F}_0$ and $\mathbf{M}_0$, and if the absolute difference between the two is smaller than a predefined tolerance, $\varepsilon = 10^{-10}$, the algorithm has converged, otherwise the algorithms in Matlab®'s *fsolve.m* function are used to iteratively update the initial guess until convergence occurs.

The red elements in Figure 5 are added to the algorithm to cope with and investigate a range of issues related to the use of a numerical approach for this particular problem. First of all, the numerical approach will only be able to find a solution if a solution truly exists. As mentioned in the introduction, it is important to realize that the heliogyro cannot create just any force and/or moment. For example, a desired force needs to belong to the force bubbles shown in Figure 3 and Figure 4 (for a pure collective or cyclic profile, respectively) in order for a solution to exist. Furthermore, from Figure 4a for a cyclic profile it is clear that for $\gamma = 0$ some $\left(F_s, F_l\right)$-combinations do not exist (a similar infeasibility region exists for the half-p profile). To cope with this issue, the desired force and moment, $\mathbf{F}_0$ and $\mathbf{M}_0$, will initially be generated by the forward mapping of a given or randomly selected set of blade pitch controls, $\mathbf{x}_0$, to ensure that a set of blade pitch controls exists that can deliver $\mathbf{F}_0$ and $\mathbf{M}_0$. Subsequently, the robustness of the numerical technique may be an issue, which (for the current problem) can be expressed through how sensitive the algorithm is to the initial guess. From the forward mapping of $\mathbf{x}_0$ it is known that $\mathbf{x}_0$ is (one of) the solution(s) to $\mathbf{F}_0$ and $\mathbf{M}_0$. Therefore, when providing $\mathbf{x}_0$ as an initial guess to the numerical solver, i.e., $\hat{\mathbf{x}}_0 = \mathbf{x}_0$, the solver will converge on the initial iteration. To find the sensitivity of the algorithm to the initial guess, the initial guess is perturbed by an amount $\Delta\mathbf{x}$, i.e., $\hat{\mathbf{x}}_0 = \mathbf{x}_0 + \Delta\mathbf{x}$, and this paper investigates for what values of the perturbation, $\Delta\mathbf{x}$, the solver still converges.

Another issue related to the numerical character of the solver is how to know which blade pitch controls to choose in order to generate the desired force and/or moment. Again, as demonstrated in Figure 4a, a cyclic profile may not be able to generate just any value for $\mathbf{F}_0$ and/or $\mathbf{M}_0$ and no *single* solution may exist as already became clear from the solution to the simplified collective Sun-facing case in Eqs. (6) and (7). This issue can partly be tackled by common sense. For example, when the aim is to find a particular force without inducing any moments, a cyclic profile may be chosen. Alternatively, if the main task of the blade pitch is to spin-up or spin-down the heliogyro or to deploy the heliogyro blades, a simple collective strategy may be chosen (more details on specific attitude control tactics can be

found in Reference [7]). However, when multiple force or moment components are required, or the heliogyro is not facing the Sun, combinations of blade pitch controls may have to be considered to find *a* solution or the most desirable solution. The final section of this paper, Section VIII, applies this common sense approach to a designed trajectory, but first (throughout Sections V to VII) a particular set of blade pitch controls is assumed (e.g., a pure collective profile, a pure cyclic profile, or a profile employing all five controls).

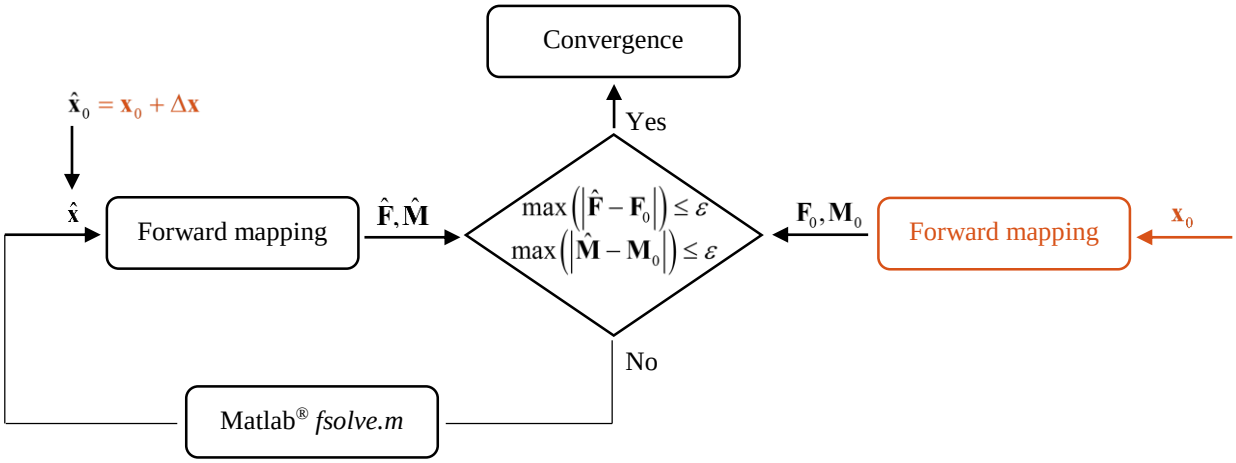

Figure 5 Schematic of numerical inverse algorithm.

V. Results - Inverse problem for SRP force

This first section of results applies the numerical approach described in Section IV to find the blade pitch controls that generate a desired SRP force. Different profiles are considered, including a collective-only and a cyclic-only profile.

A. Collective-only profile

Starting with a relatively simple case, Figure 6 provides the results for a collective profile and assuming that the heliogyro is at a Sun-facing attitude ($\eta = \gamma = 0^o$). Note that this problem has an analytical solution (see Section III), but is used here to get a first impression of the performance of the numerical solver. The horizontal axis considers a range of values for the variable $\mathbf{x}_0$, i.e., the collective profiles that are used to create desired force vectors, $\mathbf{F}_0$, onto which the numerical solver has to converge. The vertical axis indicates by how much the initial guess is perturbed from $\mathbf{x}_0$ (in the range $\Delta\mathbf{x} \in \left[-90^o, 90^o\right]$) and white and gray areas indicate unsuccessful and successful convergence of the numerical solver, respectively.

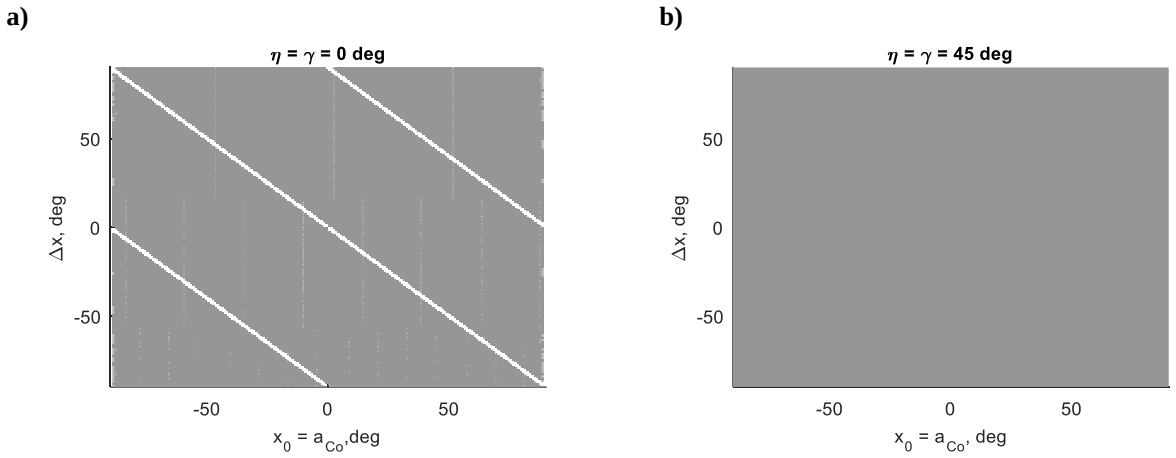

Figure 6 Performance of numerical inverse problem on SRP force only for *collective* profile. White and gray areas indicate unsuccessful and successful convergence, respectively.

The results in Figure 6a show that the numerical approach works very well, allowing convergence for very bad initial guesses (that are up to 90° perturbed from the solution), except for a few cases that are represented by the diagonal white lines in Figure 6a. In those cases, the initial guess is very close or equal to a collective amplitude of 90° for which the heliogyro does not generate any SRP force and as a result, the algorithm finds it difficult to move away from the initial guess, i.e., it gets trapped in a local minimum.

Additional results are presented in Figure 6b for a non-Sun-facing attitude of the heliogyro ($\eta = \gamma = 45^o$). Exactly the same procedure as for the case $\eta = \gamma = 0^o$ is adopted, this time with immaculate performance. In this case, initial guesses close to 90° do not cause any problems due to the non-Sun-facing attitude of the heliogyro.

Finally, rather than fixing the heliogyro's attitude, the attitude can be assumed to be part of the inverse problem (i.e., $\hat{\mathbf{x}} = \begin{bmatrix} \eta & \gamma & a_{Co} \end{bmatrix}$), which can become of importance when a generic three-dimensional force vector needs to be provided by the collective profile without any information on what attitude might be capable of producing that force. Therefore, 250 combinations of collective amplitudes and attitudes are randomly selected from a uniform distribution within the domains $a_{Co} \in \left[-90, 90^o\right]$, $\eta \in \left[-90, 90^o\right]$, and $\gamma \in \left[-90, 90^o\right]$. Each combination of $\mathbf{x}_0 = \begin{bmatrix} \eta & \gamma & a_{Co} \end{bmatrix}$ is mapped forward to generate 250 values for $\mathbf{F}_0$ and the 250 values for $\mathbf{x}_0$ are perturbed in the range $\Delta\mathbf{x} = \left[-45^o, 45^o\right]$. The 250 randomly selected profiles, $\mathbf{x}_0$, are provided in Figure 7, where they are sorted in ascending order to show that the domains are properly sampled.

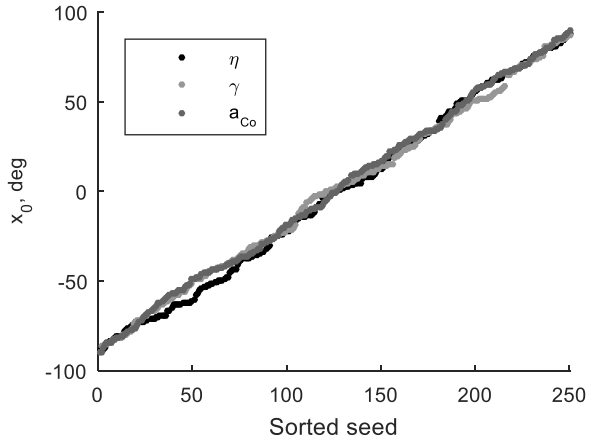

Figure 7 Randomly selected collective amplitudes, a_{Co}, and heliogyro attitude angles η and γ, sorted in ascending order.

When solving this particular inverse problem, use can be made of some further insights into the problem. Let's first focus on the clock angle γ. For the collective profile, the effect of the clock angle γ is a rotation of the two-dimensional SRP force curves around the $\hat{\mathbf{s}}$-axis over an angle equal to γ, see Figure 3d. The angle γ can therefore easily be obtained from the transverse, F_l, and out-of-plane, F_p, force components as:

$$\gamma = \tan^{-1}\left(\frac{F_p}{F_l}\right). \tag{9}$$

Note that the angle γ can be defined on the interval $\gamma = \left[-90^o, 90^o\right]$ as it defines the orientation of the force-*plane*, again see Figure 3d. Values for γ outside this domain can be captured with a change in sign of the angle η. This is demonstrated in Figure 8a, where the force combinations marked with '1' exist for $(\eta, \gamma, a_{co}) = \left(-32^o, 25^o, 20^o\right)$ while the force combinations marked with '2' exist for $(\eta, \gamma, a_{co}) = \left(-32^o, 25^o + 180^o, 20^o\right)$, but also for $(\eta, \gamma, a_{co}) = \left(32^o, 25^o, 20^o\right)$.

The remaining two variables, a_{co} and η can be obtained by solving the following nonlinear system for a_{co} and η:

$$\begin{aligned} F_s(\eta, \gamma = 0, a_{co}) &= F_{0,s} \\ F_l(\eta, \gamma = 0, a_{co}) &= \sqrt{{F_{0,l}}^2 + {F_{0,p}}^2} \end{aligned} \tag{10}$$

Because the angle γ can be obtained analytically (as per Eq. (9)), Eq. (10) reduces the three-dimensional problem to a two-dimensional problem, i.e. in the gray force-plane of Figure 8c) by setting $\gamma = 0$. In this gray force plane the desired force components are $F_{0,s}$ and $\sqrt{F_{0,l}^2 + F_{0,p}^2}$, as also illustrated in Figure 8c).

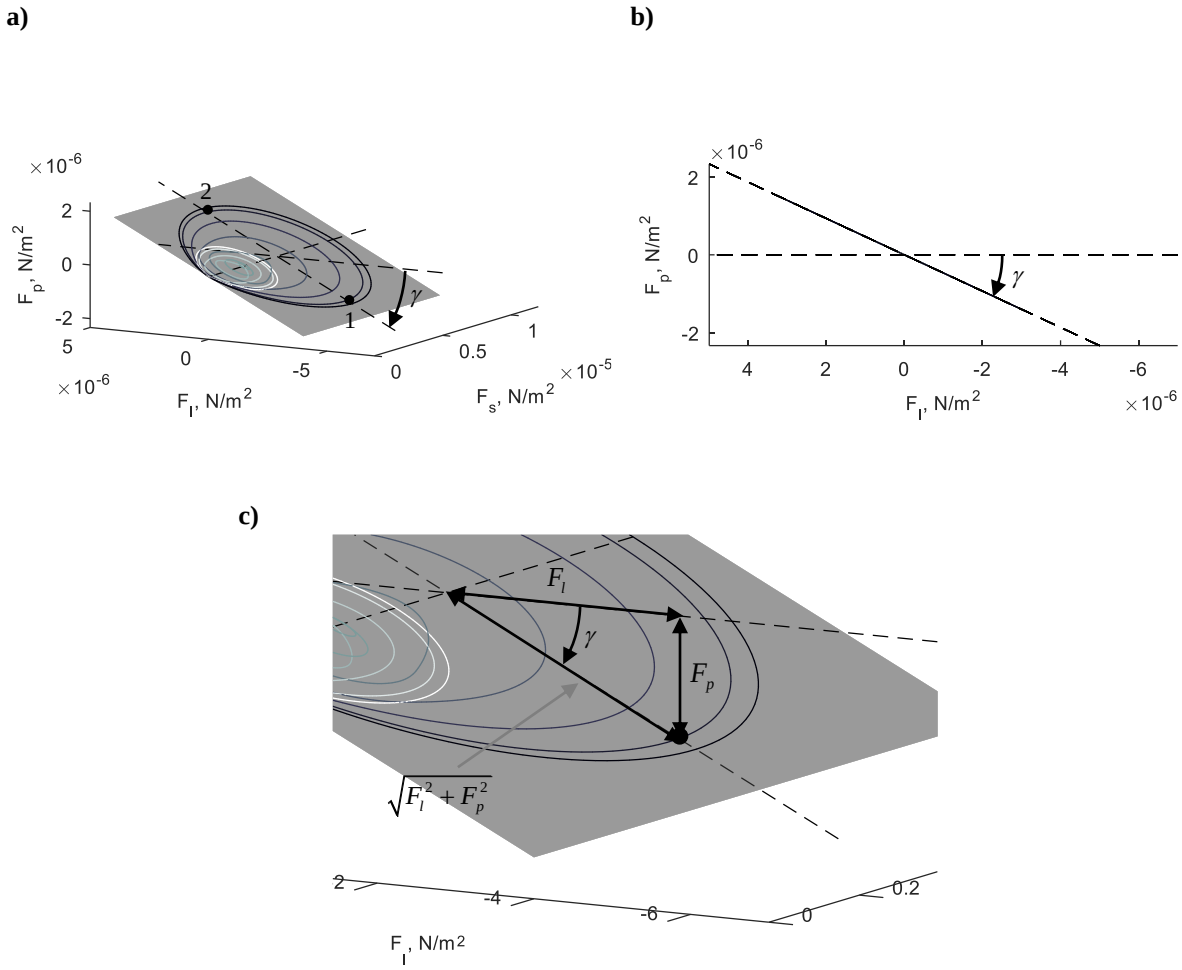

Figure 8 Illustration to support inverse problem definition. a) Force curves for a range of collective amplitudes for γ = 25°. b) (F_l,F_p)-view of subplot a). c) Detail of subplot a).

The results of the inverse problem are shown in Figure 9. Subplot a) provides similar information as for a fixed attitude in Figure 6 only now with the 250 runs over the randomly selected control profiles, $\mathbf{x}_0 = [\eta \quad \gamma \quad a_{Co}]$, along the horizontal axis. The white regions in Figure 9a, especially those close to the boundaries on $\Delta\mathbf{x}$, show the impact of the additional controls of the cone and clock angles, η and γ, as the algorithm does not always converge. To eliminate some of the randomness of the problem set-up, Figure 9b is added to show what percent of the 250 runs converges for each value for $\Delta\mathbf{x}$. Clearly, if $\Delta\mathbf{x} = 0°$, i.e. the initial guess is not perturbed with respect to the known solution, all runs converge. But even for initial guesses that are within -33° to +28° of the solution, 90 percent of the runs converge. This means that, if no information on the potential solution is available, the domains of η, γ, and a_{Co} only need to be sampled a few times to ensure convergence of the numerical algorithm. For example, the domains for η, γ, and a_{Co} each span 180°, which can be divided into three sub-domains each spanning 60° (to cover the -33° to +28° domain). If each of these subdomains is sampled, convergence of the algorithm can almost be guaranteed. The

result in Figure 9b also shows a symmetry around the value $\Delta\mathbf{x} = 0°$, which indicates that the direction (positive or negative) in which the initial guess is perturbed does not *on average* influence the performance of the numerical solver.

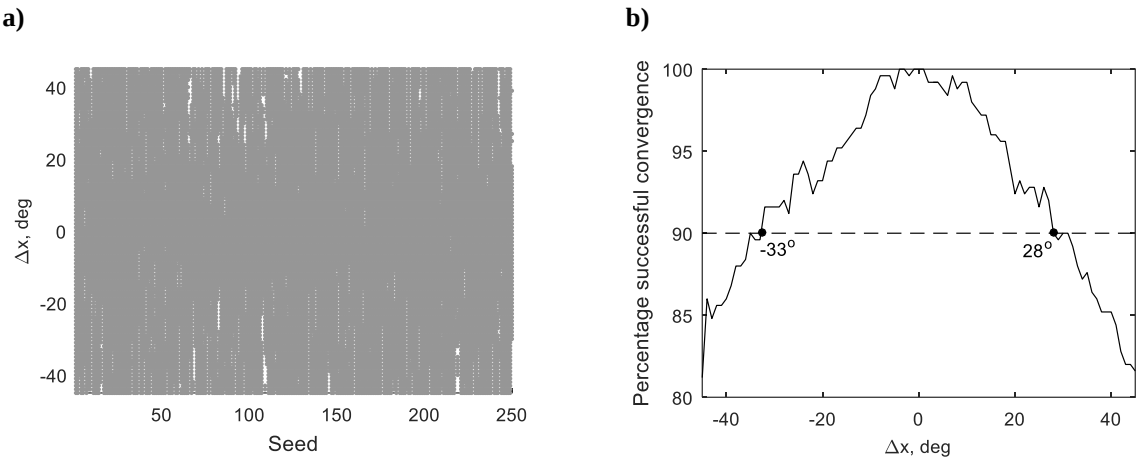

Figure 9 Performance of numerical inverse problem on SRP force only for *collective* profile and heliogyro attitude. a) White and gray areas indicate unsuccessful and successful convergence, respectively. b) Percentage successful convergence per value for Δx.

B. Cyclic-only profile

A similar approach to the one described for a collective profile can be applied to the use of a cyclic profile. When starting with a fixed attitude of the sail (either $\eta = \gamma = 0°$ or $\eta = \gamma = 45°$), 250 control profiles, $\mathbf{x}_0 = \begin{bmatrix} a_{Cy} & \phi_{Cy} \end{bmatrix}$, are randomly sampled within the domains $a_{Cy} \in \left[-90^o, 90^o\right]$ and $\phi_{Cy} \in \left[-180^o, 180^o\right]$ and perturbed in the range $\Delta\mathbf{x} = \left[-90^o, 90^o\right]$. The performance of the numerical solver is presented in Figure 10a and b in a similar fashion as in Figure 9 for a collective profile. The figures first of all show that the attitude of the heliogyro has little influence on the performance of the numerical algorithm. Furthermore, when comparing the results in Figure 10a and b with those in Figure 6 for the collective profile, it can be concluded that the increase in number of controls for the cyclic profile causes a decrease in performance compared to that of the collective profile. However, the results in Figure 10a and b still show that convergence is almost guaranteed if the initial guess is within ±55° of the solution, requiring only very few samples across the domains for a_{Cy} and ϕ_{Cy} to ensure convergence if no information on the solution is available. Additional results are presented in Figure 10c for the case that the heliogyro's attitude is considered part of the inverse problem, i.e., $\mathbf{x}_0 = \begin{bmatrix} \eta & \gamma & a_{Cy} & \phi_{Cy} \end{bmatrix}$. Note that the approach in Eq. (10) cannot be applied here, because no clear relation between γ and the three-dimensional force vector exists for the cyclic profile, see Figure 4b. The problem thus has to be solved as a full three-dimensional problem. Although the impact of the additional controls, η and γ,

becomes clear from comparing Figure 10a and b with Figure 10c, 90 percent of the runs converges with initial guesses that are within ± 27° of the solution.

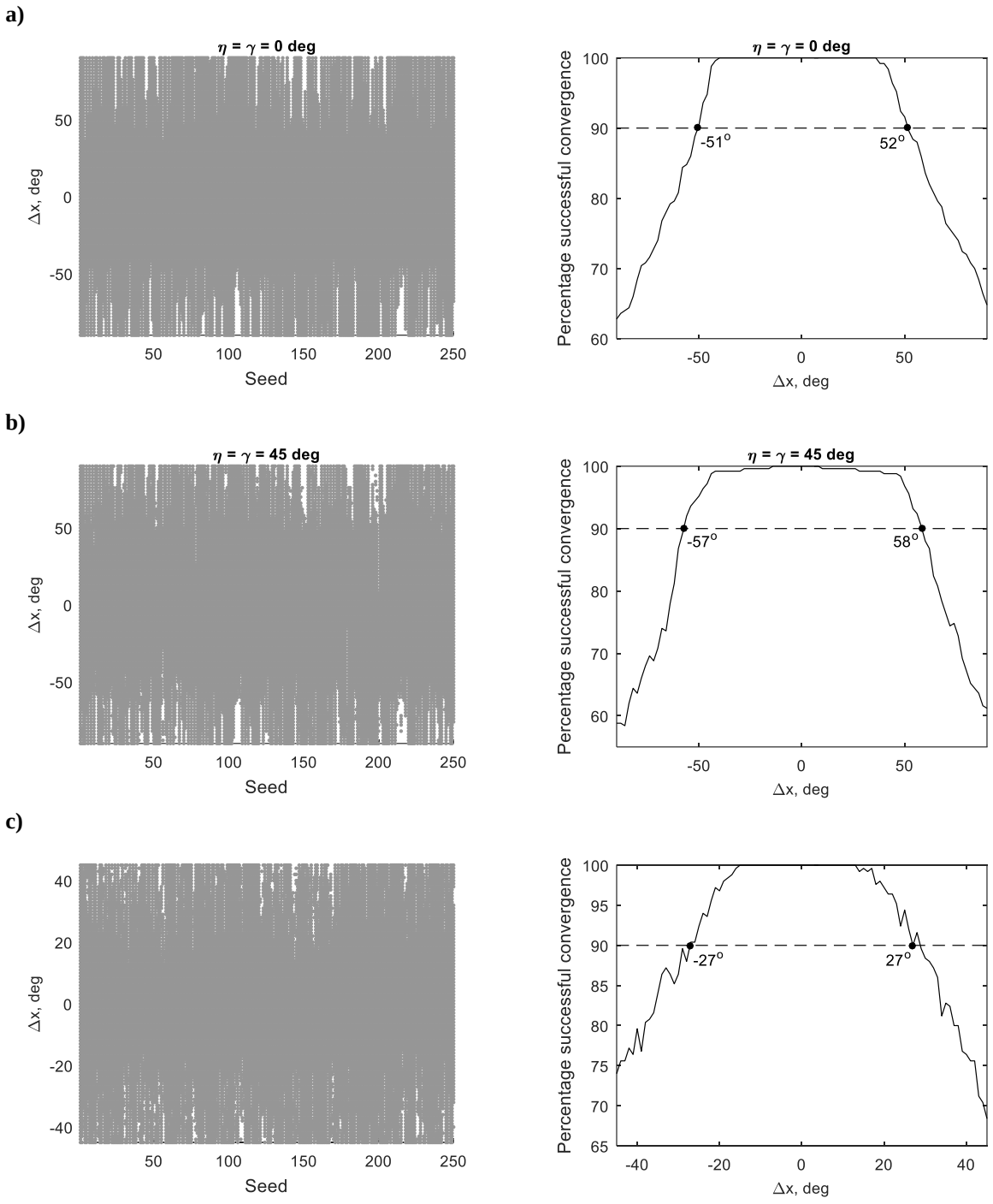

Figure 10 Performance of numerical inverse problem on SRP force only for *cyclic* profile. In the left column, white and gray areas indicate unsuccessful and successful convergence, respectively, and the right column shows the percentage successful convergence per value for Δx. a) $\eta = \gamma = 0°$. b) $\eta = \gamma = 45°$. c) η and γ are part of inverse problem.

VI. Inverse problem for SRP moment

Similar to the inverse problem for the SRP force only, the numerical algorithm can also be applied to find the heliogyro blade pitch controls that generate a desired moment. Reference [7] already investigated in great detail a set of specific attitude tactics that reflect typical heliogyro operations (e.g. spin and precession tactics), providing the required pitch profile to meet a range of desired moments. This paper will complement the work in Reference [7] by investigating the pitch profile required to generate any moment for any attitude of the heliogyro, applying the numerical scheme of Section IV in exactly the same way as was done in Section V for an SRP force only.

Because the cyclic profile does not generate any moment and the collective profile has already been considered in quite some detail in Section V, this section will focus on the use of the half-p profile. The results for a fixed attitude of the sail are provided in Figure 11a and b; however, note that γ has no influence on the moments in the $D\left(\hat{\mathbf{d}}_1,\hat{\mathbf{d}}_2,\hat{\mathbf{d}}_3\right)$ frame. The only difference between Figure 11a and b is thus the value for η, where $\eta = 0$ only generates moments around the $\hat{\mathbf{d}}_2$- and $\hat{\mathbf{d}}_3$-axes, while $\eta \neq 0$ generates moments around all body axes. The reduction in the performance of the numerical solver between the cases $\eta = 0$ and $\eta = 45^o$ (90 percent convergence for $\Delta\mathbf{x} = \left[-29^o, 32^0\right]$ and $\Delta\mathbf{x} = \left[-22^o, 26^o\right]$, respectively) thus shows the effect of an increase in the number of equations (i.e., from two to three). The results in Figure 11c further increase the dimensionality of the problem, by adding the cone angle, η, as control (again, the angle γ is not considered because it does not affect the moments in the $D\left(\hat{\mathbf{d}}_1,\hat{\mathbf{d}}_2,\hat{\mathbf{d}}_3\right)$ frame), with a further reduction in the performance as a result.

As a final comparison, the red lines in the right column of Figure 11 are the results for a collective profile only. Because the collective profile reduces the number of controls and equations by one compared to the half-p profile, a better performance can be observed.

a)

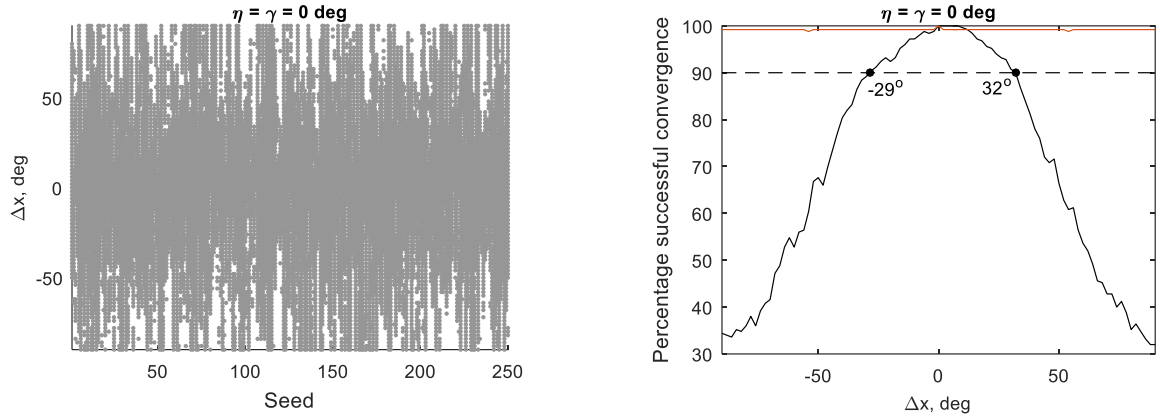

b)

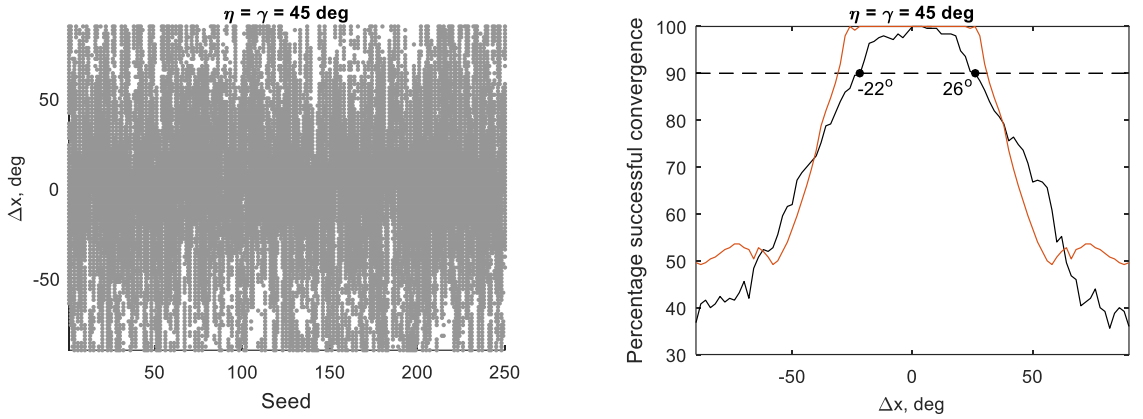

c)

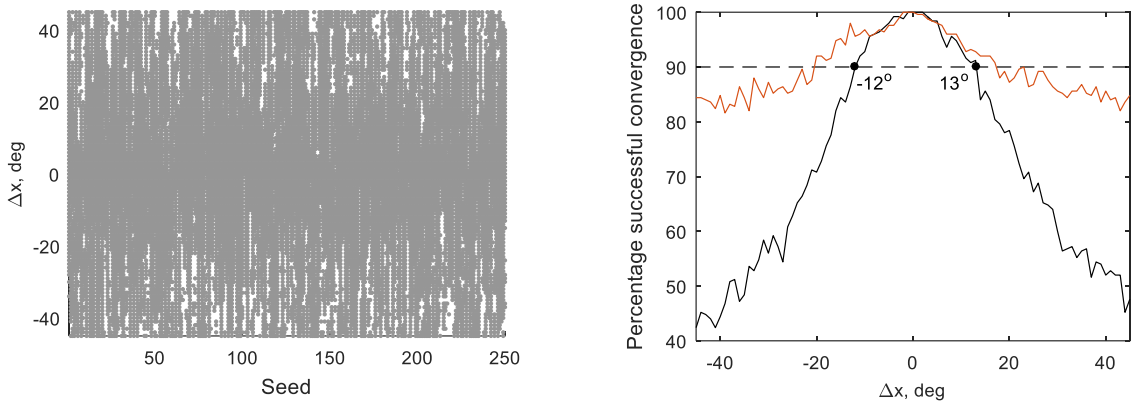

Figure 11 Performance of numerical inverse problem on SRP moment only for *half-p* profile (red results in right column are for a *collective* profile). In left column, white and gray areas indicate unsuccessful and successful convergence, respectively, and the right column shows the percentage successful convergence per value for Δx. a) $\eta = \gamma = 0°$. b) $\eta = \gamma = 45°$. c) η and γ are part of inverse problem.

VII. Inverse problem for coupled SRP force and moment

The last case to investigate is the inverse problem for the fully couple SRP force *and* moment, i.e., finding the blade pitch controls that provide both a desired force and a desired moment. This problem can be investigated for each pitch profile separately (collective, cyclic and half-p), but to limit the number of results presented, this section will only consider the case where *all* pitch controls are used simultaneously. When fixing the heliogyro's attitude, this results in five pitch controls, $\hat{\mathbf{x}} = \begin{bmatrix} a_{Co} & a_{Cy} & \phi_{Cy} & a_{HP} & \phi_{HP} \end{bmatrix}$, to solve for six equations (three force components and three moment components). When also including the attitude of the heliogyro, the number of controls increases to seven.

The results for a fixed attitude of the sail are provided in Figure 12a and b and show a relatively good performance of the numerical solver, when considering that 90 percent of the runs converge for $\Delta\mathbf{x} = \begin{bmatrix} -13^o, 17^o \end{bmatrix}$ and $\Delta\mathbf{x} = \begin{bmatrix} -13^o, 16^o \end{bmatrix}$, respectively. These domains for $\Delta\mathbf{x}$ are approximately half those for the collective, force-only, free heliogyro attitude case in Figure 9, while the number of controls and equations between these two cases has scaled up from three to five and three to six, respectively. These results would imply a nearly linear scaling in how well the initial guess has to be for the numerical solver to converge. Furthermore, when comparing Figure 12a and b it becomes clear that the attitude of the heliogyro has very limited influence on the performance of the linear solver, much less influence than for the cases considered for the force-only or moment-only in Sections V and VI. From the results in Figure 12c it can be even be concluded that *adding* the attitude to the inverse problem can have a positive effect as 90 percent of the runs converge for $\Delta\mathbf{x} = \begin{bmatrix} -18^o, 19^o \end{bmatrix}$.

a)

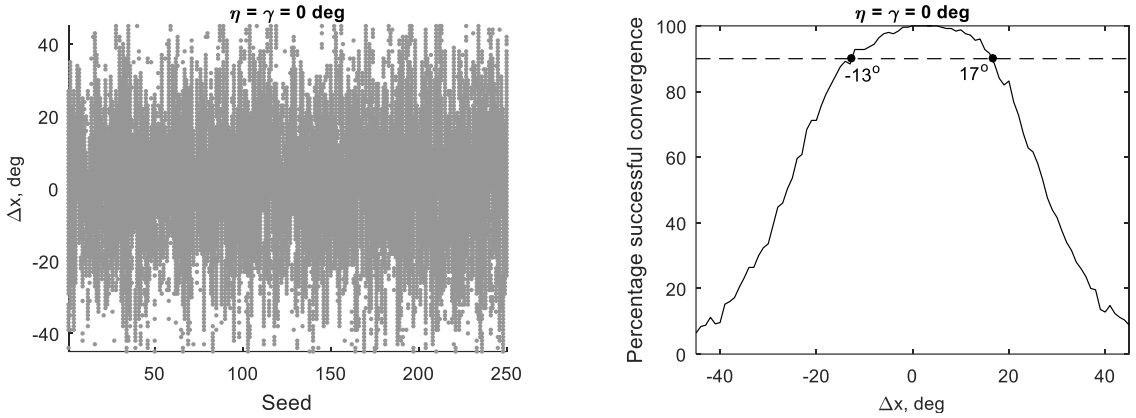

b)

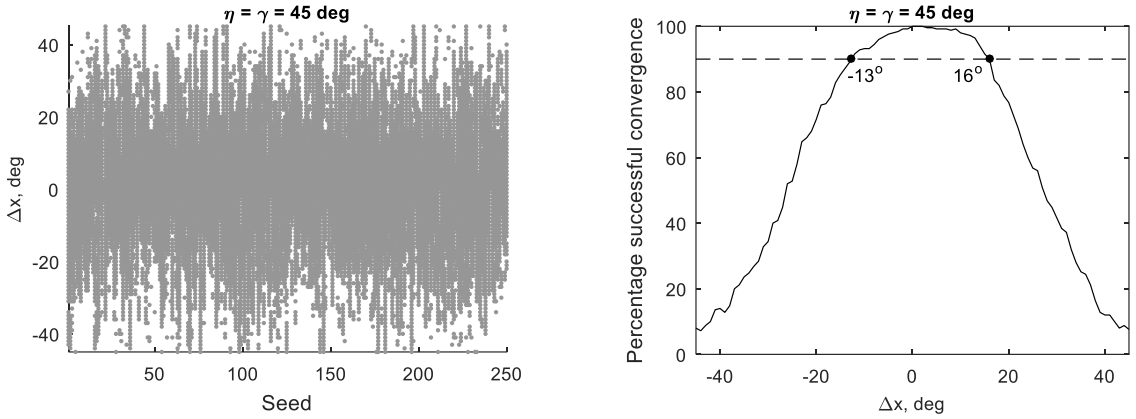

c)

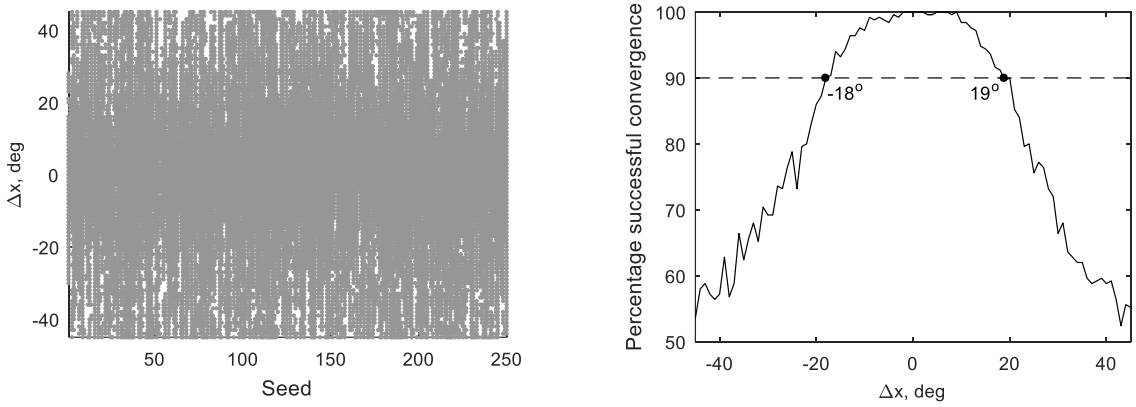

Figure 12 Performance of *coupled* force and moment numerical inverse problem for *all pitch profiles* combined. In left column, white and gray areas indicate unsuccessful and successful convergence, respectively, and the right column shows the percentage successful convergence per value for Δx. a) $\eta = \gamma = 0°$. b) $\eta = \gamma = 45°$. c) η and γ are part of inverse problem.

VIII. Application to reference trajectory

In this final part of the paper, the insights obtained and algorithms developed in the previous sections are applied to a reference trajectory. In particular, References [6, 9] present a range of heliogyro trajectories that enable recovery from injection errors into a solar sail Sun-Earth sub-L_1 halo orbit. Displaced halo orbits can be created by exploiting the solar radiation pressure acting on a solar sail and have been proposed for several mission concepts (e.g., Geostorm [11] and Sunjammer [12]). Details on how to generate these orbits are omitted here for brevity, but they can be found in a range of references, including References [13-15]. These references show that displaced halo orbits exist for different sail steering laws, e.g., a steering law where the sail's attitude remains perpendicular to the axis connecting the Sun and Earth or a Sun-facing steering law where the sail's attitude remains perpendicular to the Sun-sail line. In this paper, the latter steering law is adopted for a sail with a characteristic acceleration of 0.2153 mm/s^2 (the performance of the previously proposed Sunjammer mission [12]), where the characteristic acceleration is the acceleration created by the sail when facing the Sun at 1 AU distance from the Sun. The corresponding displaced halo orbit is presented in Figure 13a (in the synodic Sun-Earth $C\left(\hat{\mathbf{x}},\hat{\mathbf{y}},\hat{\mathbf{z}}\right)$-reference frame), which also indicates the nominal injection point and the actual injection point (i.e., including an injection error). The halo orbit considered has an orbital period of approximately 270 days, in- and out-of-plane amplitudes of approximately 1.5 million km and 450,000 km, respectively, and an injection error of 500,000 km in position and 130 m/s in velocity is applied in the direction of the unstable eigenvector. To recover the nominal halo orbit, a linear-quadratic regulator (LQR) feedback controller is used as per the analyses in References [6, 9]. The LQR feedback controller returns the solar sail accelerations required to maneuver the heliogyro back onto the nominal halo orbit. Important to note is that the LQR feedback controller is built in such a way that the requested accelerations are constrained to the volume enclosed by the force bubbles of Figure 3 and Figure 4, ensuring that a blade pitch profile exists that can provide the requested accelerations. Also important to note is that the heliogyro is slightly 'oversized', i.e., its characteristic acceleration is slightly larger than that needed to generate the nominal orbit: 0.2213 mm/s^2. This is done to improve the heliogyro's orbital control authority. However, the larger characteristic acceleration implies that, once the nominal orbit is recovered, a Sun-facing steering law of the heliogyro (for which the halo orbit was designed) would produce too much acceleration and the blades of the heliogyro will need to be pitched in order to reduce the acceleration it produces. The result of the LQR feedback controller is provided as the acceleration components in the $S\left(\hat{\mathbf{s}},\hat{\mathbf{l}},\hat{\mathbf{p}}\right)$-frame, see the solid lines in Figure 13b. Note that the time on the horizontal axis is provided as the number of revolutions in the nominal halo orbit.

In this section, the inverse problem for the trajectory in Figure 13a and b is to find the heliogyro's attitude and blade pitch profile that provides the accelerations in Figure 13b. For this, a cyclic profile is selected, as it does not generate a net torque (see Section II). The numerical approach to obtain the heliogyro's attitude and cyclic profile is exactly as detailed in Section IV and Figure 5, only replacing the red elements on the right-hand side of Figure 5 by the accelerations (or, equivalently, forces) of Figure 13b. Furthermore, from the analyses in Section V.B. it is clear that the inverse algorithm can be initiated with a relatively inaccurate initial guess, allowing the red elements in the top-left corner of Figure 5 to be replaced by a trial-and-error method at the initial time. For subsequent time steps, a

continuation approach is used, where the solution at the previous time step is used as an initial guess for the current time step.

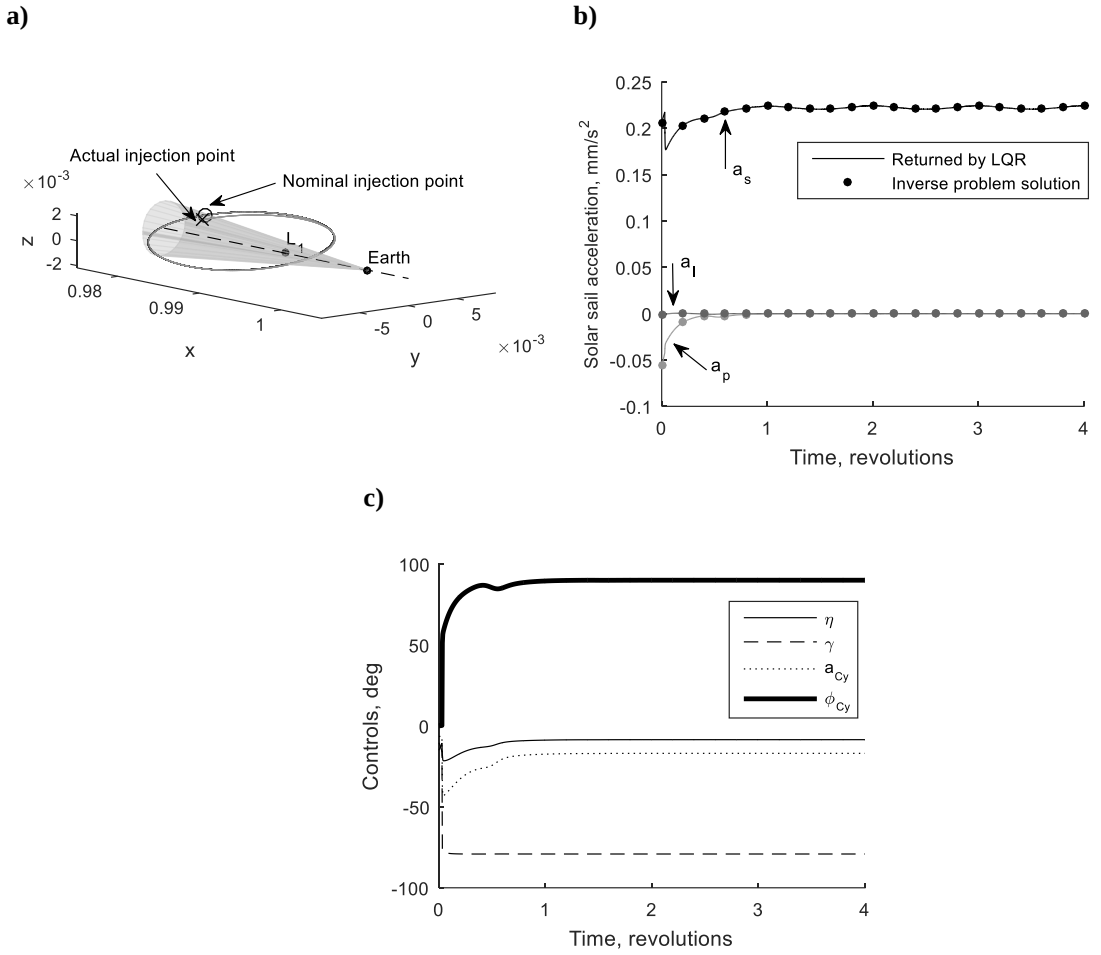

Figure 13 Inverse problem solution for SRP acceleration for control of solar sail halo orbit. a) Trajectory. b) Acceleration components requested by LQR controller (lines) and from solution of inverse problem (markers). c) Attitude and cyclic pitch profile controls.

The result of the inverse problem in terms of the heliogyro's attitude (angles η and γ) and cyclic pitch profile (amplitude a_{Cy} and phase ϕ_{Cy}) is shown in Figure 13c. Furthermore, for verification purposes, the markers in Figure 13b indicate the acceleration components that follow from a forward mapping of the inverse solution, which agree with what the LQR feedback controller requested. The control profiles in Figure 13c furthermore show that a rapid change in blade pitch and attitude is required to track the acceleration in the first few days of the recovering trajectory. Once the orbit is recovered, the controls converge to a solution close to $\hat{\mathbf{x}} = \begin{bmatrix} \eta & \gamma & a_{Cy} & \phi_{Cy} \end{bmatrix} = \begin{bmatrix} -8.5^o & -79.1^o & -17.0^o & 90^o \end{bmatrix}$. Again, note that the inverse problem does not converge to a Sun-facing steering law as this would produce too much acceleration. A constant cyclic pitch of -17° is used to

reduce this acceleration together with a cone angle, η, and phase angle of the cyclic pitch profile, ϕ_{Cy}, to ensure that the cyclic profile only produces a force along the Sun-sail line. Note that the value for γ is arbitrary for a force along the Sun-sail line only.

Future work will focus on finding an additional pitch profile to provide the moments necessary to track the heliogyro's attitude as presented in Figure 13c. Because this pitch profile may in turn produce an SRP acceleration, it must be noted that it must be designed such that, combined with the SRP acceleration produced by the cyclic profile in the above, the desired SRP acceleration of Figure 13b is generated.

Conclusions

This paper has provided and assessed a numerical approach to solving the heliogyro's inverse problem. The solution to the inverse problem provides the required heliogyro blade pitch (as well as heliogyro attitude in some cases) to produce a desired SRP force and/or moment. As with many numerical approaches, the algorithm requires an initial guess and the performance of the numerical approach is quantified by how good that initial guess needs to be in order to converge onto the solution. A range of test cases are considered, selecting either a single pitch profile (collective, cyclic or half-p) or a combination thereof and considering only the inverse problem for the SRP force or moment or the fully coupled force + moment problem. The results show that the numerical solver performs extremely well for simple, low-dimensional problems. For example, for the case where a collective profile is the only control and the inverse problem for the SRP force-only is solved, the algorithm converges to a solution for initial guesses for the collective amplitude angle that are within $\pm 90°$ of the solution. When increasing the dimensionality by adding the heliogyro's attitude angles as controls, the performance decreases, but the algorithm still converges if the initial guess is within $\pm 30°$ of the solution. Therefore, if no knowledge or insights about the solution is available, the full domains for each control only need to be sampled at few locations to find an initial guess for which the algorithm converges. When increasing the dimensionality even further, up to the maximum where all five controls are involved to create a coupled SRP force & moment, the performance is at its worst, but it still allows convergence for initial guesses within approximately $\pm 15°$ of the solution. Finally, the algorithm has been applied to find the heliogyro pitch controls that can deliver the accelerations required to follow a reference trajectory, in particular a trajectory that will bring the heliogyro back onto a nominal solar sail Sun-Earth sub-L_1 halo orbit after injection errors into the orbit. A cyclic profile has been shown to be able to provide the desired accelerations for a particular attitude profile of the heliogyro.

Acknowledgements

Jeannette Heiligers would like to acknowledge the support of the Marie Skłodowska-Curie Individual Fellowship 658645 - S4ILS: Solar Sailing for Space Situational Awareness in the Lunar System

References

1. McInnes, C.R., "Solar Sailing: Technology, Dynamics and Mission Applications," *Springer-Praxis Books in Astronautical Engineering*, Springer-Verlag, Berlin, 1999.
2. Vulpetti, G., Johnson, L., and Matloff, G.L., "Solar Sails A Novel Approach to Interplanetary Travel, 2nd Edition," *Springer-Praxis Books in Space Exploration*, 2nd ed., Springer Science+Business Media, New York, 2015.
3. Macdonald, M. and McInnes, C., "Solar Sail Science Mission Applications and Advancement," *Advances in Space Research*; Vol. 48, No. 11, 2011, pp. 1702-1716. doi: 10.1016/j.asr.2011.03.018
4. MacNeal, R.H., "Helicopters for Interplanetary Space Flight," *34th National Forum of the American Helicopter Society*, American Helicopter Soc., Washington, D.C., 1978.
5. Wilkie, W.K., Warren, J.E., Guerrant, D.V., Lawrence, D.A., Gibbs, S.C., Dowell, E.H., Heaton, A.F., Juang, J., Horta, L.G., Lyle, K.H., Littell, J.D., Bryant, R.G., Thomson, M.W., and Walkemeyer, P.E., "Heliogyro Solar Sail Research at NASA," *Advances in Solar Sailing*, Springer Praxis-Books - Astronautical Engineering, Berlin, 2013, pp. 631-650.
6. Heiligers, J., Guerrant, D., and Lawrence, D., "Heliogyro Orbital Control Authority," *International Symposium on Space Flight Dynamics* Munich, Germany, 2015.
7. Guerrant, D. and Lawrence, D., "Tactics for Heliogyro Solar Sail Attitude Control Via Blade Pitching," *Journal of Guidance, Control, and Dynamics*; Vol. 38, 2015, pp. 1785-1799. doi: 10.2514/1.G000861
8. Guerrant, D. and Lawrence, D., "Nonlinear Torsional Dynamics and Control of Heliogyro Solar Sail Blades (AIAA 2015-0435)," *2nd AIAA Spacecraft Structures Conference*, Reston, Virginia, USA, 2015.
9. Heiligers, J., Guerrant, D., and Lawrence, D., "Exploring the Heliogyro's Superior Orbital Control Capabliities for Solar Sail Halo Orbits," *Journal of Guidance, Control, and Dynamics, Under Review*; Vol., 2016
10. MacNeal, R.H., "The Heliogyro - an Interplanetary Flying Machine (Report: NASA-CR-84460)," United States, 1967.
11. West, J.L., "The GeoStorm Warning Mission: Enhanced Opportunities Based on New Technology," *14th AAS/AIAA Spaceflight Mechanics Conference*, AAS-04-102, Maui, Hawaii, 2004.
12. Heiligers, J., Diedrich, B., Derbes, B., and McInnes, C.R., "Sunjammer: Preliminary End-to-End Mission Design," *2014 AIAA/AAS Astrodynamics Specialist Conference*, San Diego, CA, USA, 2014.
13. McInnes, A.I.S., "Strategies for Solar Sail Mission Design in the Circular Restricted Three-Body Problem," M.S. Dissertation, Purdue University, School of Aeronautics and Astronautics, West Lafayette, 2000.
14. Nuss, J.S., "The Use of Solar Sails in the Circular Restricted Problem of Three Bodies," M.S. Dissertation, Purdue University, West Lafayette, 1998.
15. Baoyin, H. and McInnes, C., "Solar Sail Halo Orbits at the Sun-Earth Artificial L1-point," *Celestial Mechanics and Dynamical Astronomy*; Vol. 94, 2006, pp. 155-171. doi: 10.1007/s10569-005-4626-3